



## ORIGINAL ARTICLE

# Are Developmental Trajectories of Cortical Folding Comparable Between Cross-sectional Datasets of Fetuses and Preterm Newborns?

Julien Lefèvre<sup>1,2</sup>, David Germanaud<sup>3,4,5,6,7,†</sup>, Jessica Dubois<sup>8,9,10,†</sup>, François Rousseau<sup>11</sup>, Ines de Macedo Santos<sup>12</sup>, Hugo Angleys<sup>8,9,10</sup>, Jean-François Mangin<sup>12</sup>, Petra S. Hüppi<sup>13,14</sup>, Nadine Girard<sup>15,16</sup>, and François De Guio<sup>12,17</sup>

<sup>1</sup>Aix-Marseille Université, CNRS, ENSAM, Université de Toulon, LSIS UMR 7296, 13397 Marseille, France, <sup>2</sup>Institut de Neurosciences de la Timone UMR 7289, Aix Marseille Université, CNRS, 13385 Marseille, France, <sup>3</sup>Service de Neurologie Pédiatrique et Pathologie Métabolique, APHP, Hôpital Robert Debré, DHU PROTECT, 75019 Paris, France, <sup>4</sup>Université Paris Diderot, Sorbonne Paris Cité, 75013 Paris, France, <sup>5</sup>CEA, NeuroSpin, UNIACT, UNIPEDIA, 91191 Gif-sur-Yvette, France, <sup>6</sup>INSERM, U1129, 75015 Paris, France, <sup>7</sup>Université Paris Descartes, Sorbonne Paris Cité, 75006 Paris, France, <sup>8</sup>Cognitive Neuroimaging Unit, INSERM, U992, 91191 Gif-sur-Yvette, France, <sup>9</sup>NeuroSpin Center, CEA, 91191 Gif-sur-Yvette, France, <sup>10</sup>University Paris Sud, 91400 Orsay, France, <sup>11</sup>Institut Mines-Telecom, Telecom Bretagne, INSERM U1101 LaTIM, 29609 Brest, France, <sup>12</sup>CEA, NeuroSpin Center, UNATI, 91191 Gif-sur-Yvette, France, <sup>13</sup>Department of Pediatrics, Geneva University Hospitals, 1211 Genève 14, Switzerland, <sup>14</sup>Department of Neurology, Children's Hospital, Harvard Medical School, Boston, MA 02115, USA, <sup>15</sup>Aix Marseille Université, CNRS, CRMBM UMR 7339, 13385 Marseille, France, <sup>16</sup>Service de Neuroradiologie, Hôpital de La Timone, 13005 Marseille, France and <sup>17</sup>Université Paris Diderot, Sorbonne Paris Cité, UMR-S 1161 INSERM, 75010 Paris, France

Address correspondence to Julien Lefèvre. Email: julien.lefevre@univ-amu.fr

<sup>†</sup>David Germanaud and Jessica Dubois contributed equally to this work.

## Abstract

Magnetic resonance imaging has proved to be suitable and efficient for *in vivo* investigation of the early process of brain gyrification in fetuses and preterm newborns but the question remains as to whether cortical-related measurements derived from both cases are comparable or not. Indeed, the developmental folding trajectories drawn up from both populations have not been compared so far, neither from cross-sectional nor from longitudinal datasets. The present study aimed to compare features of cortical folding between healthy fetuses and early imaged preterm newborns on a cross-sectional basis, over a developmental period critical for the folding process (21–36 weeks of gestational age [GA]). A particular attention was carried out to reduce the methodological biases between the 2 populations. To provide an accurate group comparison, several global parameters characterizing the cortical morphometry were derived. In both groups, those metrics provided good proxies for the dramatic brain growth and cortical folding over this developmental period. Except for the cortical volume and the rate of sulci appearance, they depicted different trajectories in both groups suggesting that the transition from *in utero* to *ex utero* has a visible impact on cortical morphology that is at least dependent on the GA at birth in preterm newborns.

**Key words:** cortical surface, curvature, development of cortical sulci, fetal MRI, in utero, morphometry, premature birth, segmentation

## Introduction

Cortical folding is a major process of human brain development that mostly occurs during fetal life. The development of primary sulci is observed from around 14 weeks of gestational age (GA), secondary sulci from 32 weeks GA and tertiary sulci from 39 weeks GA (Chi et al. 1977). Several postmortem studies have been conducted to bring some insights into the understanding of gyral and sulcal formation (Chi et al. 1977; Zhang et al. 2010, 2011; Zhan et al. 2013) but the whole cortical folding process remains largely unknown. Explaining interindividual variability is a challenge for models and theories (Regis et al. 2005; Lefevre and Mangin 2010; Toro 2012; Bayly et al. 2014; Tallinen et al. 2014). There is a growing need for group studies at early developmental stages taking into account individual structural variability to infer subtle abnormalities due to neurodevelopmental disorders (Dubois, Benders, Borradori-Tolsa et al. 2008; Clouchoux et al. 2013). In vivo magnetic resonance imaging (MRI) makes it now possible and further enables to collect longitudinal data of particular interest when studying such a dynamic process. MRI has proved to be suitable and efficient for in vivo investigation of the early brain development in fetuses and preterm newborns as it is harmless and already offers a good tissue contrast and image resolution (Garel et al. 2001; Huppi 2011; Girard et al. 2012).

Therefore, early cortical folding studies may rely on 2 different types of MRI data, from in utero fetuses and ex utero preterm newborns. While fetuses seem the most obvious subjects, the processing steps from image acquisition to cortical gyrification assessment are not straightforward. First, MRI studies of the typically developing brain in healthy fetuses raise ethical issues since, in most countries, MRI cannot be performed on pregnant women for research purpose only (Hand et al. 2006), leading to the inclusion of clinical and potentially impaired populations. Then, fetal MRI has long been hampered by a poor image quality notably due to motion of the fetus in utero and respiration of the mother (Huppi 2011). Recent technical developments have emerged to bypass these technical difficulties, using postprocessing methods to reconstruct high-resolution motion-corrected volumes from 2D fast MR sequences (Rousseau et al. 2006; Kim et al. 2010) and opening up the way to high-resolution studies of cortical folding (Habas, Kim, Corbett-Detig et al. 2010; Habas, Kim, Rousseau et al. 2010; Rajagopalan et al. 2011, 2012; Clouchoux et al. 2012; Habas et al. 2012; Wright et al. 2014). Because of less challenging motion issues, quantitative studies of cortical folding were performed earlier in preterm newborns with neonatal MRI protocols bringing innovative data for the quantification of early sulcation and suggesting its interest as a marker of development (Dubois, Benders, Borradori-Tolsa et al. 2008; Dubois, Benders, Cachia et al. 2008; Rodriguez-Carranza et al. 2008; Weisenfeld and Warfield 2009; Dubois et al. 2010; Ball et al. 2012; Gousias et al. 2012).

However, an inescapable but still unresolved question remains the comparability of cortical-related measurements derived from fetus and preterm data. Indeed, for both biological and methodological reasons, these measurements may be different, even if an inborn developmental impairment or a neurological complication associated with prematurity is excluded. So far, the developmental folding trajectories (i.e., the time-related sequence of folds development) drawn up from both

populations have not been strictly compared, neither from cross-sectional nor longitudinal datasets even if one can mention a first attempt in (Clouchoux et al. 2012). Would there be a discontinuity in the gyrification process between in utero and ex utero environments? Eventually, would it be valuable to consider as typical the folding trajectory drawn up from preterm newborns with no cerebral lesions? Those questions have been partially addressed in the study by Kapellou et al. who described that the degree of prematurity modulates scaling relationships between cortical surface area and volume in a semilogitudinal dataset (Kapellou et al. 2006). Nevertheless, the respective influence of preterm birth per se and extrauterine growth could not be disentangled so far because comparisons with healthy fetuses of equivalent ages were lacking.

The aim of the retrospective study described in this paper was to compare features of cortical folding between healthy fetuses and preterm newborns on a cross-sectional basis, over a developmental period critical for the folding process (21–36 weeks of GA). Preterm newborns were imaged shortly after birth so that long-term effects of prematurity were expected to be low. A particular attention has been carried out to reduce the methodological difference between segmentation procedures that could skew the comparison between in utero and ex utero status. To provide an accurate group comparison, several parameters characterizing the cortical morphometry were derived, such as brain volume, cortical surface area, Gyrification Index (GI), curvedness, and shape indices. Their dependence as a function of GA, brain volume, and groups were systematically assessed and discussed in terms of developmental trajectory.

## Materials and Methods

### Subjects

#### Fetuses

Subjects were retrospectively selected from the fetal clinical database acquired in the department of neuroradiology in La Timone hospital (Marseille, France) between 1 January and 31 December 2011. The local ethical committee approved the protocol and all mothers gave informed consent for the study. Fetal brain MRI was performed either when anomaly was suspected at ultrasounds, requiring further clarification for management, or systematically in patients with personal–familial history with a risk for fetal brain damage after 28 weeks GA even when ultrasounds scan appeared normal (Girard and Chaumoitte 2012). Images of abnormal fetal brains that composed most of the database were excluded from this study according to radiological criteria (all assessments performed by N.G.). Furthermore, fetuses were included if at least 3 artifact-free volumes in different orientations (axial, coronal, sagittal) had been acquired and if no disease was reported in the regular clinical follow-up. Fourteen fetuses were finally selected. GA at time of MRI acquisition varied from 21 to 34 weeks (mean age:  $29.6 \pm 3.5$  weeks).

#### Preterm Newborns

Subjects were 27 preterm newborns, most of them included in the preterm “normal” group of previous studies (Dubois, Benders, Borradori-Tolsa et al. 2008; Dubois, Benders, Cachia et al. 2008;

Dubois et al. 2010). Preterm data were acquired at Geneva University Hospitals, under a protocol approved by the local ethical committee. GA at birth varied from 25.6 to 35.6 weeks (mean age:  $30.2 \pm 2.5$  weeks), and GA at time of MRI acquisition varied from 26.7 to 35.7 weeks (mean age:  $31.4 \pm 2.4$  weeks). The MRI examination was performed as soon as possible after birth (delay between 0.1 and 3 weeks, mean:  $1.2 \pm 0.7$ , delay < 1 week for 13 newborns, delay < 2 weeks for 11 newborns). All newborns had a normal intrauterine growth (no growth restriction), were from a single pregnancy (no twin newborns), and showed normal brain appearance on MRI images obtained at birth and at term equivalent age.

#### Gestational Age Assessment

In both populations, GA was assessed from first trimester obstetric ultrasonography, which is available as a systematic public health policy in both France and Switzerland. GA was nonetheless conventionally expressed in week from the first day of the last menstrual periods.

### MRI Acquisition

#### Fetuses

In utero acquisitions were performed on a 1.5-T MRI system (Symphony TIM, Siemens; Erlangen, Germany). Mothers were sedated with Rohypnol® (flunitrazepam) to reduce motion artifacts. To reconstruct and segment fetal data, we only used  $T_2$ -weighted images acquired on axial, coronal, and sagittal planes with a half Fourier acquisition single shot turbo spin echo (HASTE) sequence with the following parameters: repetition time (TR) = 1680 ms, echo time (TE) = 135 ms, flip angle =  $180^\circ$ , number of averaging = 1, slice thickness = 3 mm, field of view (FOV) =  $380 \times 380$  cm, Matrix =  $358 \times 512$ , corresponding to a raw spatial resolution of  $0.742 \times 0.742 \times 3$  mm<sup>3</sup>.

#### Preterm Newborns

No sedation was used and the newborns were spontaneously asleep. Special “mini-muffs” were applied on their ears to minimize noise exposure. The study was conducted on 2 1.5-T MRI systems (N = 15 for Philips Medical Systems, Best, the Netherlands; N = 12 for Siemens Medical Systems, Erlangen, Germany, see Dubois et al. (2010)). Coronal slices covering the whole brain were imaged by a  $T_2$ -weighted fast spin echo sequence with the following parameters: 80 slices; no parallel imaging; echo train length (ETL) = 16, for Eclipse TE/TR = 156/4040 ms, for Intera/Achieva TE/TR = 150/4000 ms, FOV =  $18 \times 18$  cm<sup>2</sup>, matrix =  $256 \times 256$  corresponding to a spatial resolution of  $0.7 \times 0.7 \times 1.5$  mm<sup>3</sup> (Philips), and 84 slices; parallel imaging GRAPPA factor 2; ETL/Turbo factor = 15, TE/TR = 151/5700 ms, FOV =  $20 \times 20$  cm<sup>2</sup>, matrix =  $256 \times 256$  corresponding to a spatial resolution of  $0.8 \times 0.8 \times 1.2$  mm<sup>3</sup> (Siemens).

### Image Processing

#### Image Reconstruction for Fetuses

To obtain high-resolution isotropic images from low-resolution images acquired in different planes, we used the reconstruction technique described by Rousseau et al. (2006, 2013). This retrospective method is based on a registration refined compounding of multiple sets of orthogonal fast 2D MRI slices to address the key problem of fetal motion. We chose the best combination of low-resolution images based on visual quality control to exclude volumes with apparent artifacts, considering at least 3 volumes

in 3 different orientations. Final resolution of the high-resolution reconstructed volume was  $0.75 \times 0.75 \times 0.75$  mm<sup>3</sup>.

#### Cortical Surface Segmentation

For all fetuses and preterm newborns, the interface between the developing cortex and the future white matter zone, also called inner cortical surface, was segmented and reconstructed in 3D for both hemispheres independently following image postprocessing tools (Mangin et al. 2004) previously adapted to the premature newborns (Dubois, Benders, Borradori-Tolsa et al. 2008; Dubois, Benders, Cachia et al. 2008). A similar processing pipeline was used for both groups. In fetuses, input volume was the high-resolution reconstructed volume, while for preterm newborns the original MR images were analyzed. Ventricles were further eliminated and not considered in the following analyses. A smooth triangle-based mesh of the surface detected between the developing cortex and white matter zone was computed. The surface mean curvature was estimated from the mesh local geometry with positive curvatures corresponding to the gyri top, and negative curvatures to the folds bottom. Cortical meshes were checked and manual corrections were performed locally to better delineate the cortex in regions with weak tissue contrast. The procedure was elaborated by a consensus strategy between 2 operators (I.D.M.S. and J.D.) for fetuses and preterm newborns during a training session on 3 different subjects. Since the mean absolute coefficients of variation among operators for the training subjects were very low (0.26% for the total cortical surface S, 0.21% for the total inner volume V), possible variations among groups were not expected to depend on the operator expertise.

#### Medial Face Segmentation

In all fetuses, the segmentation of the medial face was not reliable enough due to poor tissue contrast. This problem was also encountered in most preterm newborns but to a lesser extent (Dubois, Benders, Cachia et al. 2008). To provide comparable sets of cortical surface for both fetuses and preterm newborns, the same operator (J.D.) delineated a curve separating medial and lateral faces (including ventral and vertex faces) using Surfpaint Toolbox (Le Troter et al. 2012) in Anatomist (<http://brainvisa.info/>). To compute a volume corresponding to the lateral surface, we defined a mesh where medial surface was completely flattened by using extensive smoothing. More precisely, the heat equation with fixed boundary conditions was applied for each of the 3 coordinates of points that corresponded to the medial surface, and the partial differential equation was solved thanks to finite element method (Allaire 2005).

#### Morphometric Analysis

To characterize cortical development in the 2 groups, we computed different global indices over each hemisphere:

1. The original volume (V) was defined as the volume inside the mesh of the inner cortical surface, computed from discrete Green–Ostrogradski formula (Lefèvre et al. 2013).
2. The truncated volume ( $V_{tr}$ ) was the volume inside the mesh with flattened medial surface. This volume was used as a measure of brain size, as justified at the beginning of the Results section, and will be referred as “volume” in the following.
3. The lateral surface area ( $S_{lat}$ ) was obtained by summing all elementary triangle areas of the mesh excluding the medial surface and corresponding to the truncated volume.
4. A global GI was derived from a local GI (Toro et al. 2008) which was defined at each point of the cortical mesh, as the ratio

between the area of the cortical surface included in a ball of radius  $R$  and the area if the cortex was flat (i.e.,  $\pi R^2$ ). Here, we implemented 2 corrections related to the application of the local index to the developing brain. First, at each point for which the ball included parts of medial surface, we only considered the area of external cortical surface and corrected the expected area  $\pi R^2$  by removing the portion of disk corresponding to medial surface. Second, to tackle brain size growth issue, we adapted the radius  $R$  of the ball so that  $10R$  equals the length of the brain in the rostro-caudal direction ( $R$  ranges from 6.6 to 9.5 mm for preterm newborns, 5.1 to 9.7 mm for fetuses). This choice was motivated by considerations on the average order of magnitude of gyral width in order to remove the effect of growth on the morphological geometry of the brains. Finally, the global GI was obtained by integrating values of local GI on the lateral surface.

- We further derived 4 global quantities from surrogates of local principal curvatures known as curvedness and shape index which provide complementary information on the cortical folding geometry (Awate et al. 2008). At each point of the cortical mesh, curvedness represents the power of folding (positive value) while shape index is a scale-invariant value canonically normalized between  $-1$  and  $+1$  that describes the local aspect of the surface (see Fig. 1). Sulci and gyri correspond to a value below  $-0.5$  and above  $0.5$ , respectively.

Histograms of curvedness and shape index on a cortical mesh have characteristic shapes (see Fig. 2). We modeled curvedness distribution by a gamma distribution of parameters  $a$  and  $b$ :

$$f(x; a, b) = \frac{1}{\Gamma(a)b^a} x^{a-1} \exp(-x/b),$$

where  $\Gamma$  is the Gamma function.

Since  $a$  and  $b$  are not intuitive to understand at a first glance, we further considered, as a global measure of the folding intensity, the peak of the gamma distribution  $c = (a - 1)b$ .

Shape index distribution was modeled by a mixture of 2 beta distributions whose general form on interval  $[0,1]$  is

$$g(x; \alpha, \beta) = \frac{\Gamma(\alpha + \beta)}{\Gamma(\alpha)\Gamma(\beta)} x^{\alpha-1} (1-x)^{\beta-1} \text{ of parameters } \alpha \text{ and } \beta$$

Since the shape index is bounded between  $-1$  and  $+1$ , beta distribution was well adapted, which is not the case for a Gaussian or a Gamma distribution. Moreover, the location of its peak is given by

$$s = \frac{\alpha - 1}{\alpha + \beta - 1}$$

For the shape index distribution, we introduced 3 parameters of interest which are easily interpreted in terms of cortical geometry: the peaks  $s_1$  and  $s_2$ , which represented the shape modes of sulci and gyri, respectively, and the proportion  $p$  of its first beta components which represented the proportion of sulci.

The parameters of interest and their physical interpretation are summarized in Table 1.

In a population of 3D objects, the relationship between any geometrical parameters (e.g., length, area, shape) and size (often identified as volume) is well modeled by a power law with exponent " $a$ ." Under the theoretical hypothesis that shape and proportion do not change with size, the value of the " $a$ " exponent is often known, for instance it is  $2/3$  for surface area. Table 1 shows theoretical scaling under this null hypothesis for each parameter of the study. If real " $a$ " is different from the theoretical one then the scaling is "allometric," meaning that shape changes with size. Allometry may be dynamic (or developmental) if size is mainly related to age as in our study, or static if size variation is due to age-independent size polymorphism (Cheverud 1982).

## Statistical Analysis

For all parameters of interest, analyses of covariance (ANCOVA) were used to quantify the interaction of group factor (fetuses vs. preterm newborns) and independent variables such as GA or volume on dependent variables (volume, surface, GI, and the 4 parameters derived from curvedness and shape index). Volume was taken in logarithmic scale to test expected allometric relationships that are best fitted by the power law model  $y = bV_{tr}^a$  (equivalent to the linear model  $\log(y) = a\log(V_{tr}) + \log b$ ) where  $y$  is a dependent variable, and  $a$  and  $b$  unknown (Im et al. 2008; Germanaud et al. 2012). Parameter " $a$ " is called scaling exponent referring to the power law model (or slope referring to the linear model in logarithmic scale). All the tested variables are supposed to have different theoretical scaling laws with brain size (see

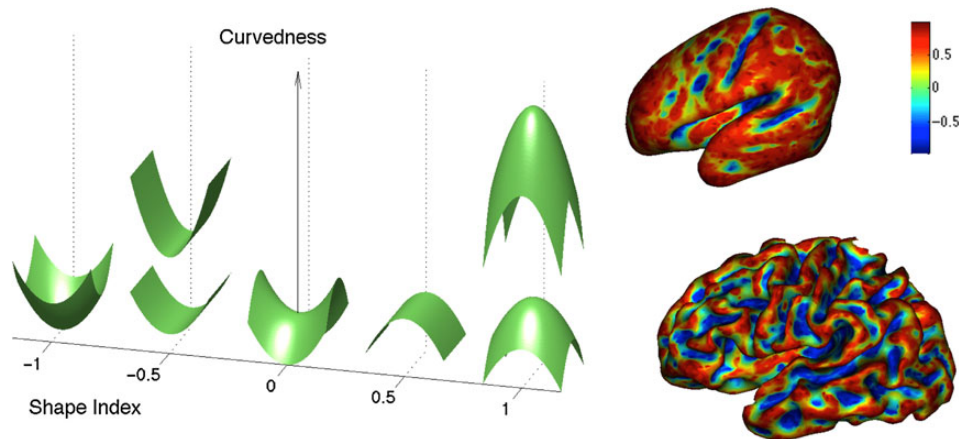


**Figure 1.** Left: Schematic representation of Curvedness and Shape Index. As for the latter parameter, values  $-1$  and  $-0.5$  describe, respectively, a sulcal pit and an archetypal sulcus, while values  $1$  and  $0.5$  represent, respectively, a local bump and an archetypal gyrus. Right: Shape Index for 2 different preterm brains (26.7 GA and 35.7 GA). The colormap is the same in both cases.

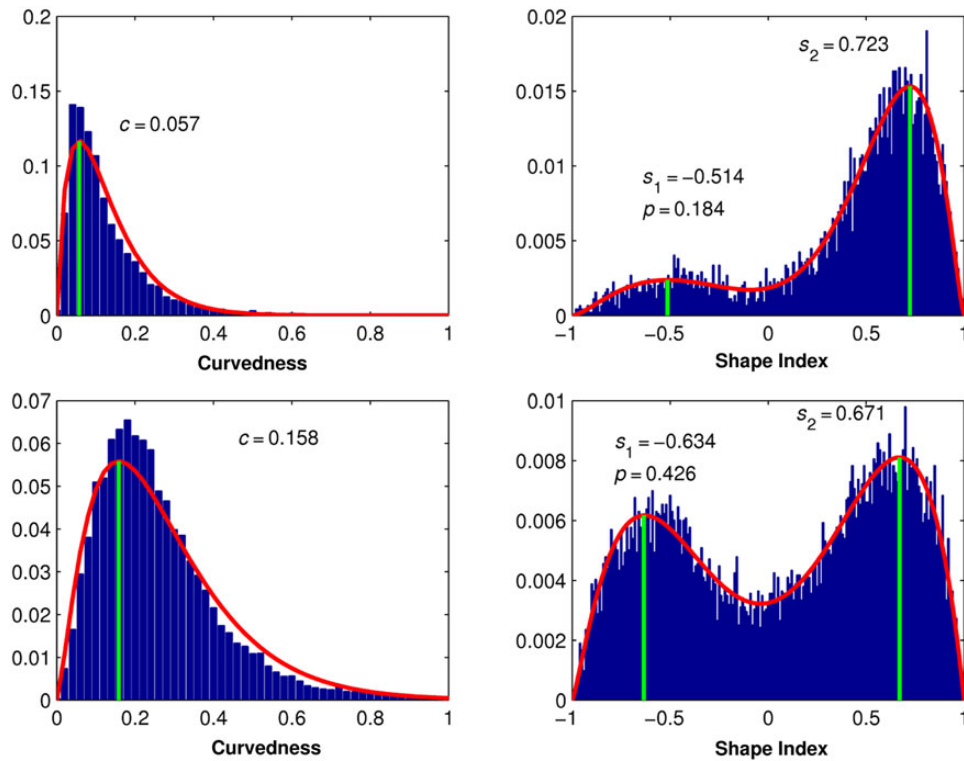


**Figure 2.** First column: histograms of curvedness for the smallest preterm brain and the biggest one (26.7 and 35.7 GA cd Fig. 1). Second column: histograms of Shape Index for the same subjects. Red curves indicate the fit by a gamma distribution and a mixture of 2 beta distributions, respectively. Green lines represent the distributions' modes. Note that the increase in value  $p$  from the first to second line (smallest to biggest brain) mainly corresponds to a rise of the first peak in the Shape Index distribution.

**Table 1** Parameters of interest, their definitions, physical interpretation, and how they theoretically scale when all axis are scaled by a factor  $\lambda$  (artificial zoom)

Indices	Definition	Scaling by $\lambda$	$a_{th}^a$	Physical interpretation
$V_{tr}$	Volume of the mesh with flattened medial surface	$\lambda^3$	1	Brain size
$S_{lat}$	Area of the lateral surface	$\lambda^2$	2/3	Cortical surface extension
GI	Integrated Gyrfication Index	$1^b$	$0^b$	Global folding intensity = rate of sulci-buried cortical surface
$c$	Mode of the curvedness distribution	$\lambda^{-1}$	-1/3	Global folding sharpness (>0)
$s_1$	Mode of first beta distribution related to shape index	1	0	Dominant sulci aspect (between -1 and 0, -0.5 being archetypal)
$s_2$	Mode of second beta distribution related to shape index	1	0	Dominant gyri aspect (between 0 and 1, 0.5 being archetypal)
$p$	Proportion of first beta distribution	1	0	Relative importance of sulci in the cortical folding geometry

<sup>a</sup>Theoretical scaling exponent in a power law scaling model.

<sup>b</sup>Scale invariance.

Table 1), any significant difference between theoretical scaling exponent and observed one reveals an allometric scaling. Normality of variables was tested with Shapiro and Wilk's test and homoscedasticity with Bartlett's test.

Statistical analyses were performed using R software (<http://www.r-project.org/>). We tested the robustness of our analysis by examining the influence of outliers (see [Supplementary Analysis](#)).

For the 5 newly introduced parameters (GI,  $c$ ,  $p$ ,  $s_1$ ,  $s_2$ ), we also computed values on the ICBM152 adult database to provide

elements of comparison between the developing and mature stage (see [Supplementary Materials](#)).

## Results

### Qualitative Comparison of Brain Volumes and Cortical Surfaces Among Fetuses and Preterm Newborns

Image reconstructions with high-resolution were successful for all 14 fetuses (see [Supplementary Fig. 3](#) for several examples).

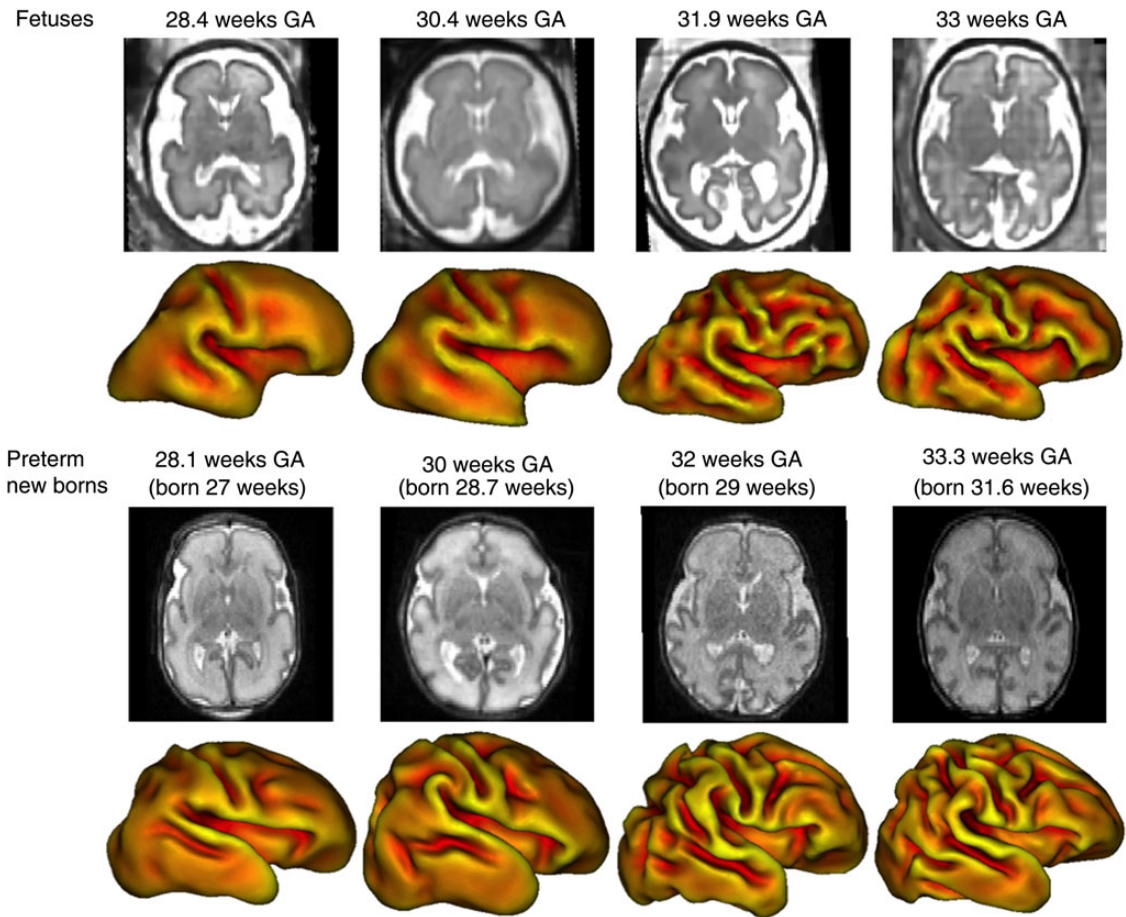


**Figure 3.** Fetal and preterm 2D images and reconstructed cortical meshes with the curvature coded in color at different gestational ages. Sulci are in red while gyri are in yellow.

Figure 3 displays a first visual comparison of fetus and preterm brains at equivalent ages. All the 2D slices and reconstructed meshes are proposed in [Supplementary Figures 1 and 2](#) to provide an exhaustive examination of the dataset. Three salient qualitative differences were observed on 2D coronal slices:

1. Cerebrospinal fluid (CSF) took a greater relative place in fetuses than in preterms, suggesting that the proportion of CSF relatively to intracranial volume is greater in fetuses than preterms. This observation was true for both pericerebral spaces and ventricles in all the studied subjects.
2. Folds looked less pronounced with more opened sulci in fetuses than in preterms, so that fetal brains looked somewhat less folded than preterm brains at equivalent ages. This observation was confirmed on reconstructed cortical surface.
3. Global shape of preterm brains looked more compact or stocky than fetal brains.

### Quantitative Comparison

All statistical results that are detailed below are summed up in [Table 2](#), showing the results of the ANCOVA models for the parameters of interest according to covariables and cofactors (group belonging: fetus or preterm). Each line corresponds to a specific model. The fit quality is expressed for each analysis in terms of percentage of variance explained by the linear model ( $R^2$ ).

The influence of the specified covariables and cofactors is highlighted by the  $F$  and  $P$  values ( $F/P$ ). There were no significant influences of outliers as shown in [Supplementary Analysis](#).

### Analyses of Volume and Lateral Cortical Surface Area

In the following analyses, we considered the truncated volume  $V_{tr}$  and the lateral cortical surface area  $S_{lat}$  as parameters of interest, because we suspected low-quality segmentations of the medial surfaces in fetuses to interfere with quantitative analysis (for equivalent truncated volumes  $V_{tr}$ , fetuses had systematically bigger original volumes than preterm newborns: effect of group on the intercept:  $F = 75.2$ ,  $P < 0.001$ ; and on slope:  $F = 4.9$ ,  $P = 0.034$ ; [Fig. 4a](#)). ANCOVA first revealed a significant effect of GA on the volume but no difference between groups for slopes and intercept ([Fig. 4b](#)), suggesting that volumetric growth was not impaired in the early imaged preterm newborns.

In contrast, taking into account the effects of age or volume, the lateral cortical surface area significantly differed between groups ([Fig. 4c,d](#)). As for the scaling exponent between surface area and volume, it showed allometric scaling in both cases (superior to the  $\frac{2}{3}$  theoretical scaling ratio between surface and volume). This allometric scaling was much higher for preterm newborns (1.23, 95% confidence interval [1.08–1.37]) than for fetuses (0.81, 95% confidence interval [0.74–0.88]), suggesting a higher cortical surface extension in the preterm group. This difference was still present even when the 2 groups were limited to common ages (subjects 26 weeks GA < age < 33.1 weeks GA,

**Table 2** Details of the statistical analyses: results of the ANCOVA models for the parameters of interest according to covariables and cofactors (group belonging: fetus or preterm)

Explained variable	$R^2$	Covariables		Group	Interaction
		GA	$\log(V_{tr})$		
$V_{tr}$	0.79	145.2/<0.001		0.1/0.71	0.2/0.68
$S_{lat}$	0.86	228.2/<0.001		10.9/0.002	15.1/<0.001
$\log(S_{lat})$	0.96		822.1/<0.001	42.3/<0.001	27.5/<0.001
GI	0.91	255.2/<0.001		89.4/<0.001	46.1/<0.001
$\log(GI)$	0.82		101.0/<0.001	60.6/<0.001	22.6/<0.001
$c^a$	0.92	356.5/<0.001		68.7/<0.001	4.6/0.039
$s_1$	0.71	71.2/<0.001		21.6/<0.001	7.4/0.01
$s_2$	0.70	87.8/<0.001		0.9/0.35	7.0/0.01
$p$	0.69	85.0/<0.001		6.8/0.013	0.0/0.92

Each line corresponds to a specific model. The fit quality is expressed for each analysis in terms of percentage of variance explained by the linear model ( $R^2$ ). The influence of the specified covariables and cofactors is highlighted by the F and P values (F/P).

<sup>a</sup>Statistical analyses for the peak of curvedness distribution (c) have been performed by removing the 2 youngest fetuses (21 and 25 weeks GA), because they were outliers in a linear model (see Fig. 5a).

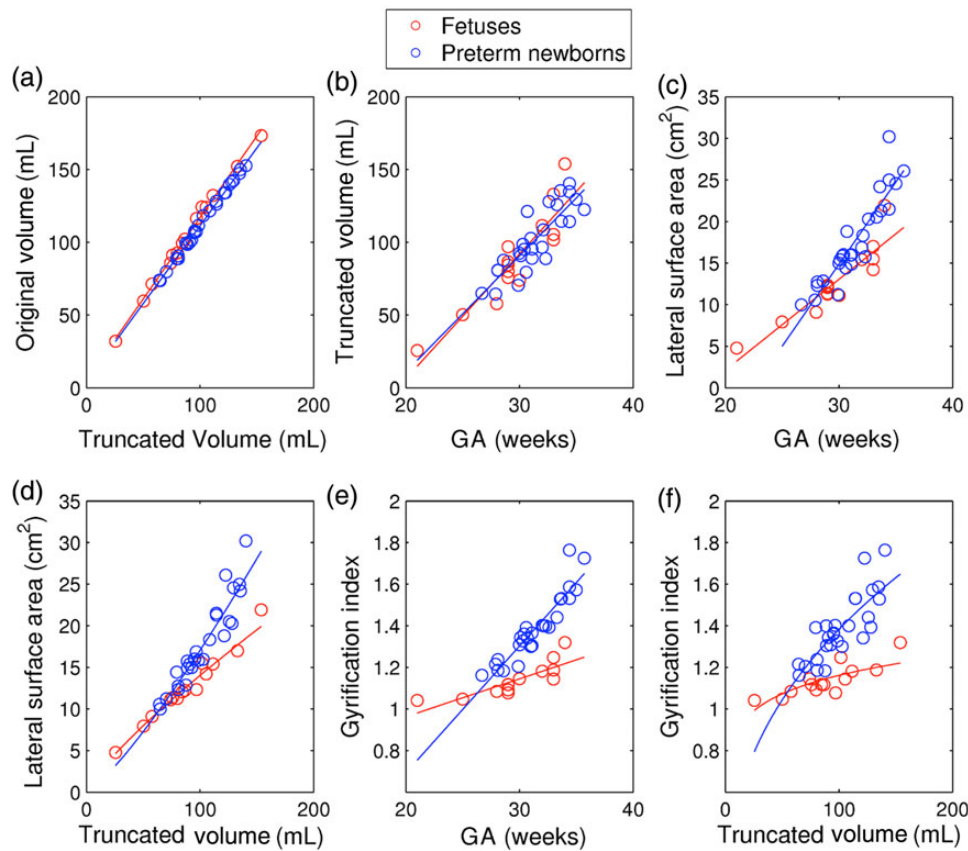


**Figure 4.** From left to right, from top to bottom: (a) Original volume as a function of truncated volume. Note that a statistical difference is present even if the lines seem very close. (b) Truncated volume as a function of gestational age. (c) Lateral cortical surface area as a function of age. (d) Lateral surface area as a function of truncated volume (allometric model/original scale). (e) Gyrfication Index as a function of gestational age. (f) Gyrfication Index as a function of truncated volume (allometric model/original scale). Blue points correspond to preterms and red points to fetuses.

11 fetuses vs. 19 preterm newborns). Note that the surface area depended more on the volume (in logarithmic scale:  $R^2 = 0.96$ ) than on GA ( $R^2 = 0.86$ ).

#### Analyses of Gyrfication Index

Consistently with differences in surface area, preterm newborns showed higher global GI than fetuses after regressing out for GA

or volume (Fig. 4e,f). The scaling exponent with respect to volume was higher for preterm newborns (0.41 [0.29–0.52]) than for fetuses (0.11 [0.06–0.17]).

#### Analyses of Other Folding Characteristics

First, we estimated the quality of fits for curvedness and shape index distributions by computing the relative errors between

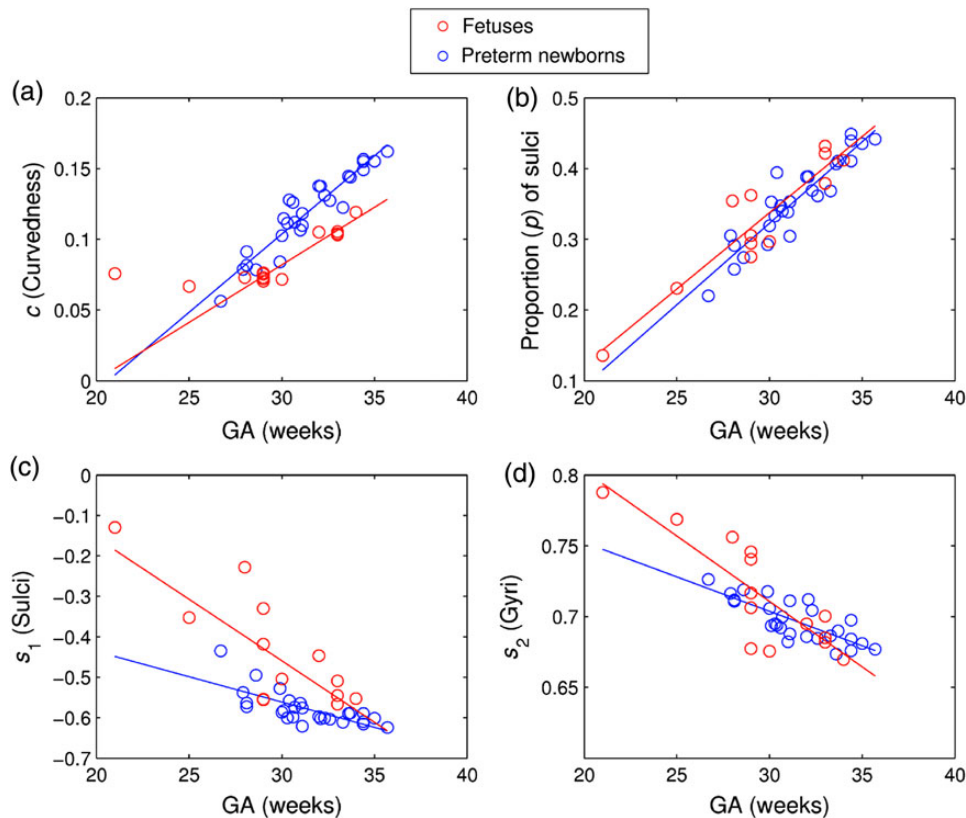


**Figure 5.** From left to right, from top to bottom: (a) Mode of curvedness distribution  $c$ . Regression line for fetuses has been computed by removing the 2 youngest fetuses (21 and 25 weeks GA). (b) Proportion of sulci ( $p$  of the beta distribution). (c) First mode of shape index distribution ( $s_1$ : sulci). (d) Second mode of shape index ( $s_2$ : gyri).

the estimated distributions and the empirical ones. For the curvedness, mean error was 1.22% (from 0.5 to 4.7%) for preterms and 4% (1.7–7.8%) for fetuses. For the shape index, mean error was 1.0% (0.7–1.4%) and 3.2% (2–4.5%), respectively. Those errors were considered satisfying to use the model in the rest of the analyses.

We further observed a systematic effect of age on the 4 global values derived from curvedness and shape index (Fig. 5). As for curvedness, the peak of gamma distribution significantly increased with age for both groups (Fig. 5a), coherently with the fact that cortical surfaces become more deeply folded with age. Preterm newborns showed a larger increase than fetuses confirming the previous results on surface area and GI. The 2 youngest fetuses were removed from this specific analysis on curvedness because they were clearly outliers and would not be relevantly fitted by a linear or strictly monotonic model. Therefore, the red regression line in Figure 5a did not take into account those 2 subjects and would have been more flat if the subjects had been included in the regression.

As for shape index, the proportion of sulci as obtained in the mixture of beta distributions showed also a significant increase with respect to age for both groups (Fig. 5b), which was coherent with the sulci appearance over this developmental period. We observed no interaction between age and groups (same slope for the 2 regression lines) even if the difference in intercept was slightly significant. Nevertheless, this difference disappeared with the removal of 2 outliers in the fetal group (see Fig. 5b age 29 weeks, 32 weeks,  $F(\text{group}) = 2.1$ , n.s.,  $F(\text{interaction}) = 0.23$ , n.s.). The absence of interaction between age and group suggests that the fetal and preterm brains showed the same proportion

of sulci according to gyri and a possible similar timeline for cortical folding pattern. Besides the proportion tended toward the empirical adult asymptote that was computed on ICBM152 database ( $0.50 \pm 0.01$ , see [Supplementary Fig. 6](#)).

The 2 modes in shape index distribution showed a significant evolution with age. The decrease of negative peak ( $s_1$ : Fig. 5c) highlighted the sulci formation from a state close to saddle ( $s_1$  about 0) to a state close to archetypal sulci ( $s_1 = -0.5$ ) and almost equal to the empirical value in adults ( $-0.63 \pm 0.01$ , see [Supplementary Fig. 6](#)), while the decrease of positive peak ( $s_2$ : Fig. 5d) demonstrated the gyri evolution from local bumps ( $s_2 = 1$ ) to archetypal gyri ( $s_2 = 0.5$  and  $0.6 \pm 0.01$  for adults, see [Supplementary Fig. 6](#)). For the 2 modes we noted an interaction between age and groups suggesting different shape aspects of the cortical surface depending on prematurity.

## Discussion

To our knowledge, this work is the first systematic comparison between cortical folding assessment from cross-sectional data in fetuses and in preterm newborns imaged shortly after birth, between 21 and 36 weeks GA, using the same image postprocessing tools. In both fetus and preterm newborn groups, we described the major effect of GA on gyrification, which is related to the dramatic brain growth and cortical folding over this developmental period. We also supported that group belonging does not affect the rate of sulci development. However, for all the other folding parameters, we found an effect of the group and an interaction between group and age, suggesting that preterm birth increases the intensity and sharpness of gyrification in

newborns, modifies the shape of gyri and sulci, but that this effect is different depending on GA. Therefore, we showed that cortical folding assessment from cross-sectional data is partly affected by ex utero preterm imaging.

### A Major Effect of GA or Size in Both Groups

The cortical surface, GI, and mode of curvedness showed very similar developmental increase in agreement with the fact that global folding intensity and sharpness both reflect the dynamic of cortical surface extension through cortical burring into folds (Garel et al. 2001; Dubois, Benders, Cachia et al. 2008; Girard and Chaumoitre 2012). The 3 other shape measures derived from curvatures were less easy to put into perspective since, to our knowledge, they have never been proposed before in the developing brain. In Batchelor et al. (2002) and in Wright et al. (2014), the authors considered also intrinsic Gaussian curvature as a measure of the total folding in elliptical regions (sulci and gyri) but they had no measures to disentangle what occurs in sulci and gyri, respectively. In this perspective, our results showed that the proportion ( $p$ ) of regions with negative curvature increased with age, and tended toward the mean adult value, which was the expected quantitative correlates to sulci emergence during early development. The 2 other measures computed ( $s_1$  and  $s_2$ ) tended to converge to values that are representative, at adult age, of the local shape of sulci and gyri, respectively. More precisely, when the brain is smooth before 25 weeks, regions with negative curvatures are very limited ( $p$  small) except for the insula whose shape contributes to predominance of saddle-like points ( $s_1$  close to 0), regions with positive curvatures are mostly isotropic ( $s_2$  not far from 1). During the cortical folding process, sulci become more abundant ( $p$  increases,  $s_1$  decreases), positive curvature regions exhibit more anisotropic pattern ( $s_2$  decreases) that correspond to gyri crests. This view on gyrification and sulcation process remains rather schematic since we considered here modal values of local shape indices. Yet, charts for such folding parameters may provide more accurate tools for the detection of nontypically developing fetuses.

Brain sizes measured by brain volume along time were comparable between our 2 groups, with 80% of size variance explained by GA, which allowed us using both parameters as predictive variable in the same way. We compared several global variables accounting for cortical complexity in relation with GA and brain volume. Age was not always the best predictor in terms of explained variance ( $R^2$ ), particularly in the case of lateral surface area. Apart from inaccuracy in GA assessment, this suggests that size may be a stronger biological determinant of some aspect of cortical geometry than GA. But the choice of a linear model with respect to GA has very limited biological explanations contrary to a power law model with respect to brain size. In their recent work, Wright et al. (2014) showed a good fit of adapted curvedness by a Gompertz growth model applied to GA. One advantage of this model is to take into account youngest fetuses whereas two of them were considered as outliers in our linear model. However, we did not consider a Gompertz model in our analysis because of the technical difficulty to include it in an ANCOVA framework that could assess differences between groups of subjects. Our results were yet compatible with those by Wright et al. in terms of order of magnitude for adapted curvedness (see Supplementary Fig. 4). Furthermore, the strong dependence between cortical surface area and volume was in agreement with the large literature on allometric relationships relying on biological models of growth (Prothero and Sundsten 1984; Toro et al. 2008).

### A Rate of Sulci Development Similar in Both Groups

The absence of group interaction on the proportion  $p$  of negative shape index values (i.e., proportion of sulci) was consistent with the fact that sulci and gyri of fetuses and preterm newborns are probably present at the same moment but not with the same amplitude and shape, confirming partially observations done in (Clouchoux et al. 2012). The developmental trajectories of this sulci proportion were very close and strictly parallel between the fetus and preterm newborn datasets. There might be a slight difference that reflects the sharpness of gyri in the fetus, consistent with the radiological observation in Figure 3, but the difference was constant, meaning not affected by the age at imaging. It would be interesting to confirm this hypothesis by studying the timing of appearance of the folds in specific regions (e.g., with methods such as Habas et al. (2012) or Wright et al. (2014)), by using surface based analysis of local folding indices (Auzias et al. 2015) or by applying recent tools of spectral analysis of gyration (Germanaud et al. 2012) among the 2 groups.

### An Age-Dependent Effect of Group on Cortical Geometry Related to Preterm Birth

If the size growth showed very similar values and trajectories between the fetus and preterm datasets, there were notable differences between the 2 situations for all the parameters describing cortical extension or folding intensity, except sulci proportion. At the same GA, the overall observation was in line with an increased cortical extension and folding intensity in preterm newborns. Indeed, for a given age or volume, fetuses were less folded than preterm newborns whatever the measure was (surface area extension, GI, or curvedness). While they were consistent with our radiological observations in Figure 3, these results seemed to be in contradiction with the only previous work comparing cortical folding between fetuses and preterm newborns (Clouchoux et al. 2012). Indeed, Clouchoux et al. found cortical plate area to be greater for fetuses than for preterm newborns at any given developmental age by comparing their fetus data to the preterm ones published by Dubois, Benders, Cachia et al. (2008). However, their comparison suffered from the difference in postprocessing procedures between the 2 datasets and, as they pointed out, from serious difference in GA computation. On the contrary, in our study, we have tried to minimize and controlled the risk of bias resulting from difference in methodology between the 2 groups: 1) data were postprocessed with the same pipeline and with good interoperator reliability between fetal and preterm groups, 2) medial cortical surface was excluded because of its lower quality of segmentation in fetuses, 3) there was no bias in age definition between our 2 groups.

In terms of dynamic scaling along the developmental time window, we found an overall allometric relationship between cortical surface area and brain volume in preterms very comparable with the one found in (Kapellou et al. 2006). More specifically, Kapellou et al. found a scaling exponent of 1.29 [1.25–1.33] over the whole range of “age at imaging” that clearly overlaps the 1.23 [1.08–1.37] exponent that we found in our “early imaged” preterm group. Otherwise, the scaling exponent we found for fetuses was much smaller, around 0.81 [0.74–0.88] which was more comparable with what is observed in the adult population for the static allometry related to brain size polymorphism (Toro et al. 2008). One of the skewing differences between the 2 groups was that fetuses were a “homogenous” group, while preterms were not because the causes of preterm birth and its consequences on the geometry of the cortical surface may be different across

extremely preterm newborns and more mature ones. The cross-sectional fit of the gyrification trajectory may then be valid in one case (fetuses) because it reflects typical developmental continuum, and skewed by a differential birth effect in the other case (preterm newborns). The fact that Kapellou et al. found the same scaling exponent in a mixed population (gathering cross-sectional and longitudinal data) as the one that we measured in a purely cross-sectional population, suggests that this bias is largely an immediate effect of preterm birth and not only due to the secondary impact of extrauterine life on cortical development. Interestingly, the authors argued convincingly for an effect of GA at birth on further cortical folding. But since authors had no references of what a normal growth in utero should be during the same developmental time window, it was difficult to disentangle the cross-sectional bias related to preterm birth supported by our results, from the true longitudinal impact of preterm birth and ex utero growth on cortical development. In that respect, the comparison between full-term born babies and extremely preterm ones imaged at full-term corrected age also seems to support such a long-lasting effect (Ajayi-Obe et al. 2000).

The effect of group and the interaction between group and GA for the shape measures derived from curvatures were consistent with the same framework of interpretation. The global folding sharpness was superior in preterm newborns than in fetuses, and this difference increased with GA. Meanwhile, the dominant shape for sulci and gyri in fetuses was always closest to the “immature” shape described above, as if preterm birth had acted as an abrupt accelerator of shape maturation. Interestingly, the age-dependent effect of preterm birth on shape diminished with GA, while it increased on folding intensity or sharpness, confirming that these 2 aspects of folding geometry are not redundant.

### Limitations Due to Acquisition and Sampling Biases

In the previous subsection An Age-Dependent Effect of Group, we mentioned 3 risks of biases that we have tried to minimize in order to obtain a more precise comparison between fetuses and preterm newborns than in Clouchoux et al. (2012). Nevertheless, we have to be explicit on the existing residual biases that cannot be disentangled in our study.

The only systematic one is the difference in acquisitions (MRI scanner coil, MRI sequence, 2D–3D processing). A direct comparison of preterm and fetal brains with a same sequence is constrained by technical and legal considerations, since HASTE sequences have high “specific absorption rates” and cannot be easily applied to preterm newborns. It is also difficult to use another common sequence between the 2 groups without damaging the quality of images, and of course a common MRI coil cannot be used neither.

The motion of fetuses or even preterm newborns is also a possible limitation. For fetal MRI, intraslice motion was minimized by sedating mothers, by using a fast acquisition strategy (HASTE sequence) and by reacquiring images until artifact-free images could be obtained. Interslice motion was handled by the registration-based approach as in Rousseau et al. (2006). For preterm newborns, motion was precisely quantified and controlled, which results in exclusion of artifacted subjects.

Laminar compartments within the cerebral wall such as the cortical plate, subplate, and intermediate zone encounter important changes during early brain development. In particular, the subplate is known to decrease from 31 weeks GA (Kostovic et al. 2002). Of note is that the changes in MRI lamination pattern are mainly caused by changes in the subplate zone (Kostovic et al. 2002). Studies comparing postmortem histological sections and

MRI scans reveal a good correlation between the compartments (Kostovic et al. 2014). Therefore, it is a good indication that our segmentation of the cortical plate and subplate is not biased or affected by the GA.

The acquisition conditions between the 2 groups can also make more difficult the delineation of the cortical mantle on in utero images as mentioned in the introduction of Clouchoux et al. (2012). The position of the gray–white interface may not be as faithful to the reality in both groups. It is also a recurrent question when dealing with gray matter/white matter interface segmentation, even in children T1-weighted imaging. But the global and large scale conformation of the folds and the sylvian fissure that are more open on MR images for fetuses supports the view of a weaker effect of acquisition than a true group effect. Future studies with higher magnetic fields would probably reveal more precision on the laminar organization of the fetal brain as already demonstrated on postmortem images (Zhang et al. 2011).

Finally, the small size of the groups, mainly the fetus one, is prone to sampling biases which make our study more sensitive to margin of errors on GA or to the fact that one subject may have been wrongly deemed typical in its development. Nevertheless, we have to recall that cohorts of fetal data are very difficult to obtain and have various sizes, 12 in (Clouchoux et al. 2012), 38 in (Habas et al. 2012); (Rajagopalan et al. 2011); and 80 in (Wright et al. 2014), in a tentative of exhaustive inventory. They correspond also to different age ranges. Moreover, the robustness of our analysis was successfully obtained by examining the influence of outliers in shape index. Finally, the consistency of several weakly correlated indices reflecting the intensity of the folding supported a true difference between our 2 groups.

### A Different Cortical Configuration Between Prenatal and Postnatal Brains?

Several previously published studies put forward a long-term developmental impairment on gyrification due to preterm birth (Ajayi-Obe et al. 2000; Kapellou et al. 2006) that may be related to differential brain maturations (Gimenez et al. 2008; Viola et al. 2011). Besides, our results on early imaged newborns strongly suggested that cortical folding in preterms is also abruptly modified by the postnatal status with respect to prenatal one in fetuses. By any means, these short-term and long-term effects seem very dependent on GA at birth and thus definitely question the reliability of cross-sectional preterm imaging to assess typical trajectory of cortical folding development. The problem of approximating extrauterine growth parameters with intrauterine ones, and the other way round, is not specific to brain or cortical development and has been raised more generally (Sauer 2007). In the context of high incidence of prematurity, there is a medical need for biological markers for preterm babies follow-up, and thus for reliable charts of cortical folding development that take into account the fact that neither prenatal fetal charts nor heterogeneous postnatal preterm charts are fully suitable. Moreover, due to the remaining technical limitations and difficulties of prenatal imaging, postnatal imaging studies in preterm babies are still very valuable, but should deal with such bias to be relevant for the understanding of typical development.

What may account for this postnatal imaging variation in the developmental trajectory of preterms? It is important to recall that morphogenesis of gyrification remains widely unexplained (Toro 2012; Bayly et al. 2014) and that several co-existing processes may contribute, solely or in concert, to the appearance of sulci. The most popular mechanisms invoked are mechanical tensions exerted by white matter fibers (Van Essen 1997) with

possibly limited influence (Xu et al. 2010); tangential extension of the cortex through intermediate radial glia cells (Reillo et al. 2011). Another hypothesis could be that the synaptogenesis has an impact on the differential gyrification observed. Results for nonhuman primates probably do not support this hypothesis since the rate of synapses production was found independent from the time of delivery (Bourgeois et al. 1989).

Anyway, these are mainly rather long-lasting effects of developmental parameters. **Supplementary Analyses** on the influence of extrauterine life indicate that preterms with less than 1 week and those with more than 1 week share the same characteristics that are distinguishable from the fetal group (see **Supplementary Analysis 2**). If one focuses on immediate changes that occur during the first 2 weeks of postnatal status and that may better account for the observed differences, one has to face that fetuses and preterm newborns live in very different physiological conditions and in different media. The change from in utero amniotic fluid to ex utero comes with abrupt modifications in physical conditions, even if the difference between amniotic pressure and atmospheric pressure is small (Fisk et al. 1992), but also in homeostatic regulation for instance of blood circulation that structurally changes (Evans and Archer 1990). These modifications are likely to influence CSF homeostasis and contribute to the greater proportion of CSF both in intra-ventricular and pericerebral spaces with respect to intracranial volume. Marginally, higher values of intrauterine pressures preceding and during labor could also modulate gyrification as they modify head molding (Lapeer and Prager 2001). Indeed, morphometric studies on preterm neonates with non-synostotic dolichocephaly have shown displacements of some major folds suggesting a link between global shape of the head and more local aspects on the cortex (Mewes et al. 2007). Additionally, the great biological stress of birth comes with stress hormones secretion from both mother and child (Gluckman et al. 1999), among which corticosteroids that are known to modify brain trophicity (Bourdeau et al. 2002). In the case of preterm birth, this biological stress is presumably higher or longer, beginning during the premature delivery threats, and in any case concerns a more vulnerable organism whose brain may be particularly sensitive to such stress. Indeed, advanced development of cortical gyrification in relation to brain growth has been suspected in chronically stressed newborns with intrauterine growth restriction (Dubois, Benders, Borradori-Tolsa et al. 2008). Likewise, there may be an additional effect of courses of antenatal corticosteroids given to accelerate fetal lung maturation. Finally, following these immediate changes, postnatal adaptation to extrauterine life goes with an important dehydration, especially in preterms (Bauer and Versmold 1989; Bauer et al. 1991), that affects the whole organism including the brain and may add up to the already mentioned modification of the brain hydric balance. A shrinking of the skull with often-transient overlap of the cranial sutures is well known by neonatologists during this period of relative physiological dehydration during which our preterm newborns were imaged.

Indeed, an even slight contraction of the skull, a decrease in relative amount of CSF, a collapse of the ventricles and perhaps a more structural modifications of the cerebral gray and white matter are among many changes that seem to occur at birth and during the following days, and that may explain an important modification in the geometric configuration of cortical folding, consistently with both our radiological observations and quantitative results. These modifications are expected to be dependent on how premature is the birth and then, to explain part of the observed interaction between group and GA that skews the extrapolation of the cortical folding developmental

trajectory from postnatal preterm newborn datasets. To model the gap between prenatal and postnatal configuration, in utero and ex utero longitudinal imaging of the same preterm and full-term newborns are still needed. More quantitative assessment of intracranial volume, CSF volume and global shape of the head should also be correlated to the modification occurring at birth. Along with longitudinal studies allowing individual modeling underneath group modeling, such perinatal studies may help disentangle the abrupt nondevelopmental effect of preterm birth from the more clinically relevant long-term effect.

To conclude, we have proposed in this work several metrics to assess and compare the cortical folding trajectories at comparable ages in 2 cross-sectional datasets, one before birth in fetuses, and the other after birth in preterm newborns of different GAs. Except for the cortical volume and the rate of sulci appearance, those metrics depicted different trajectories in each group suggesting that the transition from in utero to ex utero has a visible impact on cortical morphology and that this impact is at least dependent on the GA in preterm newborns. Our conclusions sound a note of caution on the way we approximate typical intrauterine development with extrauterine assessments, as well as how we reconstruct longitudinal trajectories from cross-sectional datasets. It also urges for further studies of the clinically relevant but still little-known cortical development in preterm babies.

## Supplementary Material

Supplementary material can be found at: <http://www.cercor.oxfordjournals.org/>.

## Funding

J.L., F.D.G., D.G., J.F.M., N.G., and J.D. are funded by the Agence Nationale de la Recherche (ANR-12-JS03-001-01, MODEGY).

## Notes

We thank the reviewers for all their helpful comments and suggestions that improve the quality of the manuscript. The authors want to thank François Leroy for his helpful advices, particularly for image segmentation. *Conflict of Interest*: None declared .

## References

- Ajayi-Obe M, Saeed N, Cowan FM, Rutherford MA, Edwards AD. 2000. Reduced development of cerebral cortex in extremely preterm infants. *Lancet*. 356:1162–1163.
- Allaire G. 2005. *Analyse numérique et optimisation*, Éditions de l'École Polytechnique, Palaiseau.
- Auzias G, De Guio F, Pepe A, Rousseau F, Mangin J-F, Girard N, Lefèvre J, Coulon O. 2015. Model-driven parameterization of fetal cortical surfaces. *Brooklyn (NY): 12th IEEE International Symposium on Biomedical Imaging (ISBI)*.
- Awate SP, Win L, Yushkevich P, Schultz RT, Gee JC. 2008. 3D cerebral cortical morphometry in autism: increased folding in children and adolescents in frontal, parietal, and temporal lobes. *Med Image Comput Assist Interv*. 11:559–567.
- Ball G, Boardman JP, Rueckert D, Aljabar P, Arichi T, Merchant N, Gousias IS, Edwards AD, Counsell SJ. 2012. The effect of preterm birth on thalamic and cortical development. *Cereb Cortex*. 22:1016–1024.
- Batchelor PG, Castellano Smith AD, Hill DL, Hawkes DJ, Cox TC, Dean AF. 2002. Measures of folding applied to the

- development of the human fetal brain. *IEEE Trans Med Imaging*. 21:953–965.
- Bauer K, Bovermann G, Roithmaier A, Gotz M, Proiss A, Versmold HT. 1991. Body composition, nutrition, and fluid balance during the first two weeks of life in preterm neonates weighing less than 1500 grams. *J Pediatr*. 118:615–620.
- Bauer K, Versmold H. 1989. Postnatal weight loss in preterm neonates less than 1,500 g is due to isotonic dehydration of the extracellular volume. *Acta Paediatr Scand Suppl*. 360:37–42.
- Bayly PV, Taber LA, Kroenke CD. 2014. Mechanical forces in cerebral cortical folding: a review of measurements and models. *J Mech Behav Biomed Mater*. 29:568–581.
- Bourdeau I, Bard C, Noel B, Leclerc I, Cordeau MP, Belair M, Lesage J, Lafontaine L, Lacroix A. 2002. Loss of brain volume in endogenous Cushing's syndrome and its reversibility after correction of hypercortisolism. *J Clin Endocrinol Metab*. 87:1949–1954.
- Bourgeois JP, Jastreboff PJ, Rakic P. 1989. Synaptogenesis in visual cortex of normal and preterm monkeys: evidence for intrinsic regulation of synaptic overproduction. *Proc Natl Acad Sci USA*. 86:4297–4301.
- Cheverud JM. 1982. Relationships among ontogenetic, static, and evolutionary allometry. *Am J Phys Anthropol*. 59:139–149.
- Chi JG, Dooling EC, Gilles FH. 1977. Gyral development of human brain. *Ann Neurol*. 1:86–93.
- Clouchoux C, du Plessis AJ, Bouyssi-Kobar M, Tworetzky W, McElhinney DB, Brown DW, Gholipour A, Kudelski D, Warfield SK, McCarter RJ, et al. 2013. Delayed cortical development in fetuses with complex congenital heart disease. *Cereb Cortex* 23:2932–2943.
- Clouchoux C, Kudelski D, Gholipour A, Warfield SK, Viseur S, Bouyssi-Kobar M, Mari JL, Evans AC, du Plessis AJ, Limperopoulos C. 2012. Quantitative in vivo MRI measurement of cortical development in the fetus. *Brain Struct Funct*. 217:127–139.
- Dubois J, Benders M, Borradori-Tolsa C, Cachia A, Lazeyras F, Leuchter RH-V, Sizonenko SV, Warfield SK, Mangin JF, Huppi PS. 2008. Primary cortical folding in the human newborn: an early marker of later functional development. *Brain*. 131:2028–2041.
- Dubois J, Benders M, Cachia A, Lazeyras F, Leuchter RHV, Sizonenko SV, Borradori-Tolsa C, Mangin JF, Huppi PS. 2008. Mapping the early cortical folding process in the preterm newborn brain. *Cereb Cortex*. 18:1444–1454.
- Dubois J, Benders M, Lazeyras F, Borradori-Tolsa C, Leuchter RHV, Mangin JF, Huppi PS. 2010. Structural asymmetries of perisylvian regions in the preterm newborn. *Neuroimage*. 52:32–42.
- Evans NJ, Archer LN. 1990. Postnatal circulatory adaptation in healthy term and preterm neonates. *Arch Dis Child*. 65:24–26.
- Fisk NM, Ronderos-Dumit D, Tannirandorn Y, Nicolini U, Talbert D, Rodeck CH. 1992. Normal amniotic pressure throughout gestation. *Br J Obstet Gynaecol*. 99:18–22.
- Garel C, Chantrel E, Brisse H, Elmaleh M, Luton D, Oury JF, Sebag G, Hassan M. 2001. Fetal cerebral cortex: normal gestational landmarks identified using prenatal MR imaging. *AJNR Am J Neuroradiol*. 22:184–189.
- Germanaud D, Lefevre J, Toro R, Fischer C, Dubois J, Hertz-Pannier L, Mangin JF. 2012. Larger is twistier: spectral analysis of gyrification (SPANGY) applied to adult brain size polymorphism. *Neuroimage*. 63:1257–1272.
- Gimenez M, Miranda MJ, Born AP, Nagy Z, Rostrup E, Jernigan TL. 2008. Accelerated cerebral white matter development in preterm infants: a voxel-based morphometry study with diffusion tensor MR imaging. *Neuroimage*. 41:728–734.
- Girard NJ, Chaumoitte K. 2012. The brain in the belly: what and how of fetal neuroimaging? *J Magn Reson Imaging*. 36:788–804.
- Girard NJ, Dory-Lautrec P, Koob M, Melani Dediu A. 2012. MRI assessment of neonatal brain maturation. *Imaging Med*. 4:613–632.
- Gluckman PD, Sizonenko SV, Bassett NS. 1999. The transition from fetus to neonate—an endocrine perspective. *Acta Paediatr Suppl* 88:7–11.
- Gousias IS, Edwards AD, Rutherford MA, Counsell SJ, Hajnal JV, Rueckert D, Hammers A. 2012. Magnetic resonance imaging of the newborn brain: manual segmentation of labelled atlases in term-born and preterm infants. *Neuroimage*. 62:1499–1509.
- Habas PA, Kim K, Corbett-Detig JM, Rousseau F, Glenn OA, Barkovich AJ, Studholme C. 2010. A spatiotemporal atlas of MR intensity, tissue probability and shape of the fetal brain with application to segmentation. *Neuroimage*. 53:460–470.
- Habas PA, Kim K, Rousseau F, Glenn OA, Barkovich AJ, Studholme C. 2010. Atlas-based segmentation of developing tissues in the human brain with quantitative validation in young fetuses. *Hum Brain Mapp*. 31:1348–1358.
- Habas PA, Scott JA, Roosta A, Rajagopalan V, Kim K, Rousseau F, Barkovich AJ, Glenn OA, Studholme C. 2012. Early folding patterns and asymmetries of the normal human brain detected from in utero MRI. *Cereb Cortex*. 22:13–25.
- Hand JW, Li Y, Thomas EL, Rutherford MA, Hajnal JV. 2006. Prediction of specific absorption rate in mother and fetus associated with MRI examinations during pregnancy. *Magn Reson Med*. 55:883–893.
- Huppi PS. 2011. Cortical development in the fetus and the newborn: advanced MR techniques. *Top Magn Reson Imaging*. 22:33–38.
- Im K, Lee JM, Lyttelton O, Kim SH, Evans AC, Kim SI. 2008. Brain size and cortical structure in the adult human brain. *Cereb Cortex* 18:2181–2191.
- Kapellou O, Counsell SJ, Kennea N, Dyet L, Saeed N, Stark J, Maalouf E, Duggan P, Ajayi-Obe M, Hajnal J, et al. 2006. Abnormal cortical development after premature birth shown by altered allometric scaling of brain growth. *PLoS Med*. 3:1382–1390.
- Kim K, Habas PA, Rousseau F, Glenn OA, Barkovich AJ, Studholme C. 2010. Intersection based motion correction of multislice MRI for 3-D in utero fetal brain image formation. *IEEE Trans Med Imaging*. 29:146–158.
- Kostovic I, Jovanov-Milosevic N, Rados M, Sedmak G, Benjak V, Kostovic-Szrentic M, Vasung L, Culjat M, Rados M, Huppi P, et al. 2014. Perinatal and early postnatal reorganization of the subplate and related cellular compartments in the human cerebral wall as revealed by histological and MRI approaches. *Brain Struct Funct*. 219:231–253.
- Kostovic I, Judas M, Rados M, Hrabac P. 2002. Laminar organization of the human fetal cerebrum revealed by histochemical markers and magnetic resonance imaging. *Cereb Cortex* 12:536–544.
- Lapeer RJ, Prager RW. 2001. Fetal head moulding: finite element analysis of a fetal skull subjected to uterine pressures during the first stage of labour. *J Biomech*. 34:1125–1133.
- Lefevre J, Intwali V, Hertz-Pannier L, Hüppi P, Mangin J-F, Dubois J, Germanaud D. 2013. Surface smoothing: a way back in early brain morphogenesis. In: Mori K, Sakuma I, Sato Y, Barillot C, Navab N, editors. *Medical image computing and computer-assisted intervention—MICCAI 2013*. Springer Berlin Heidelberg. p. 590–597.
- Lefevre J, Mangin JF. 2010. A reaction-diffusion model of human brain development. *PLoS Comput Biol*. 6:e1000749.
- Le Troter A, Auzias G, Coulon O. 2012. Automatic sulcal line extraction on cortical surfaces using geodesic path density maps. *Neuroimage*. 61:941–949.

- Mangin J-F, Rivière D, Cachia A, Duchesnay E, Cointepas Y, Papadopoulos-Orfanos D, Scifo P, Ochiai T, Brunelle F, Régis J. 2004. A framework to study the cortical folding patterns. *Neuroimage*. 23(Suppl 1):S129–S138.
- Mewes AU, Zollei L, Huppi PS, Als H, McAnulty GB, Inder TE, Wells WM, Warfield SK. 2007. Displacement of brain regions in preterm infants with non-synostotic dolichocephaly investigated by MRI. *Neuroimage*. 36:1074–1085.
- Prothero JW, Sundsten JW. 1984. Folding of the cerebral cortex in mammals. A scaling model. *Brain Behav Evol*. 24:152–167.
- Rajagopalan V, Scott J, Habas PA, Kim K, Corbett-Detig J, Rousseau F, Barkovich AJ, Glenn OA, Studholme C. 2011. Local tissue growth patterns underlying normal fetal human brain gyrification quantified in utero. *J Neurosci*. 31:2878–2887.
- Rajagopalan V, Scott J, Habas PA, Kim K, Rousseau F, Glenn OA, Barkovich AJ, Studholme C. 2012. Mapping directionality specific volume changes using tensor based morphometry: an application to the study of gyrogenesis and lateralization of the human fetal brain. *Neuroimage*. 63:947–958.
- Regis J, Mangin JF, Ochiai T, Frouin V, Riviere D, Cachia A, Tamura M, Samson Y. 2005. “Sulcal root” generic model: a hypothesis to overcome the variability of the human cortex folding patterns. *Neurol Med Chir (Tokyo)*. 45:1–17.
- Reillo I, de Juan Romero C, Garcia-Cabezas MA, Borrell V. 2011. A role for intermediate radial glia in the tangential expansion of the mammalian cerebral cortex. *Cereb Cortex*. 21:1674–1694.
- Rodriguez-Carranza CE, Mukherjee P, Vigneron D, Barkovich J, Studholme C. 2008. A framework for in vivo quantification of regional brain folding in premature neonates. *Neuroimage*. 41:462–478.
- Rousseau F, Glenn OA, Iordanova B, Rodriguez-Carranza C, Vigneron DB, Barkovich JA, Studholme C. 2006. Registration-based approach for reconstruction of high-resolution in utero fetal MR brain images. *Acad Radiol*. 13:1072–1081.
- Rousseau F, Oubel E, Pontabry J, Schweitzer M, Studholme C, Koob M, Dietemann J-L. 2013. BTK: an open-source toolkit for fetal brain MR image processing. *Comput Methods Programs Biomed*. 109:65–73.
- Sauer PJ. 2007. Can extrauterine growth approximate intrauterine growth? Should it? *Am J Clin Nutr*. 85:608S–613S.
- Tallinen T, Chung JY, Biggins JS, Mahadevan L. 2014. Gyrification from constrained cortical expansion. *Proc Natl Acad Sci USA*. 111:12667–12672.
- Toro R. 2012. On the possible shapes of the brain. *Evol Biol*. 39:600–612.
- Toro R, Perron M, Pike B, Richer L, Veillette S, Pausova Z, Paus T. 2008. Brain size and folding of the human cerebral cortex. *Cereb Cortex*. 18:2352–2357.
- Van Essen DC. 1997. A tension-based theory of morphogenesis and compact wiring in the central nervous system. *Nature*. 385:313–318.
- Viola A, Confort-Gouny S, Schneider JF, Le Fur Y, Viout P, Chapon F, Pineau S, Cozzone PJ, Girard N. 2011. Is brain maturation comparable in fetuses and premature neonates at term equivalent age? *AJNR Am J Neuroradiol*. 32:1451–1458.
- Weisenfeld NI, Warfield SK. 2009. Automatic segmentation of newborn brain MRI. *Neuroimage*. 47:564–572.
- Wright R, Kyriakopoulou V, Ledig C, Rutherford MA, Hajnal JV, Rueckert D, Aljabar P. 2014. Automatic quantification of normal cortical folding patterns from fetal brain MRI. *Neuroimage*. 91:21–32.
- Xu G, Knutsen AK, Dikranian K, Kroenke CD, Bayly PV, Taber LA. 2010. Axons pull on the brain, but tension does not drive cortical folding. *J Biomech Eng*. 132:071013.
- Zhan JF, Dinov ID, Li JN, Zhang ZH, Hobel S, Shi YG, Lin XT, Zamanyan A, Feng L, Teng GJ, et al. 2013. Spatial-temporal atlas of human fetal brain development during the early second trimester. *Neuroimage*. 82:115–126.
- Zhang Z, Liu SW, Lin XT, Sun B, Yu TF, Geng HQ. 2010. Development of fetal cerebral cortex: assessment of the folding conditions with post-mortem magnetic resonance imaging. *Int J Dev Neurosci*. 28:537–543.
- Zhang Z, Liu S, Lin X, Teng G, Yu T, Fang F, Zang F. 2011a. Development of fetal brain of 20 weeks gestational age: assessment with post-mortem magnetic resonance imaging. *Eur J Radiol*. 80:E432–E439.
- Zhang Z, Liu S, Lin X, Teng G, Yu T, Fang F, Zang F. 2011b. Development of laminar organization of the fetal cerebrum at 3.0T and 7.0T: a postmortem MRI study. *Neuroradiology*. 53:177–184.

## Supplementary materials

### **Are developmental trajectories of cortical folding comparable between cross-sectional datasets of fetuses and preterm newborns?**

Julien Lefèvre<sup>1,2</sup>, David Germanaud\*<sup>3,4</sup>, Jessica Dubois\*<sup>5</sup>, François Rousseau<sup>6</sup>, Ines de Macedo Santos<sup>7</sup>, Hugo Angleys<sup>5</sup>, Jean-François Mangin<sup>7</sup>, Petra S. Hüppi<sup>8,9</sup>, Nadine Girard<sup>10,11</sup>, François De Guio<sup>7,12</sup>

\* : Equal contribution

#### *Affiliations:*

1: Aix-Marseille Université, CNRS, ENSAM, Université de Toulon, LSIS UMR 7296, 13397 Marseille, France

2: Institut de Neurosciences de la Timone UMR 7289, Aix Marseille Université, CNRS, Marseille, France

3: APHP, Hôpital Robert Debré, DHU PROTECT, Service de Neurologie Pédiatrique et Pathologie Métabolique; Université Paris Diderot, Sorbonne Paris Cité, Paris, France

4: INSERM, U1129, Paris; CEA, NeuroSpin, UNIACT, Gif-sur-Yvette; Université Paris Descartes, Sorbonne Paris Cité, Paris, France

5: INSERM, U992, Cognitive Neuroimaging Unit; CEA, NeuroSpin Center, Gif-sur-Yvette; University Paris Sud, Orsay, France

6: ICube, Université de Strasbourg/CNRS, UMR 7357, Illkirch, France

7: CEA, NeuroSpin Center, UNATI, Gif-sur-Yvette, France

8: Geneva University Hospitals, Department of Pediatrics, Geneva, Switzerland;

9: Children's Hospital, Harvard Medical School, Department of Neurology, Boston, MA,  
USA

10: Aix Marseille Université, CNRS, CRMBM UMR 7339, Marseille, France

11: Service de Neuroradiologie, Hôpital de La Timone, Marseille 13385, France

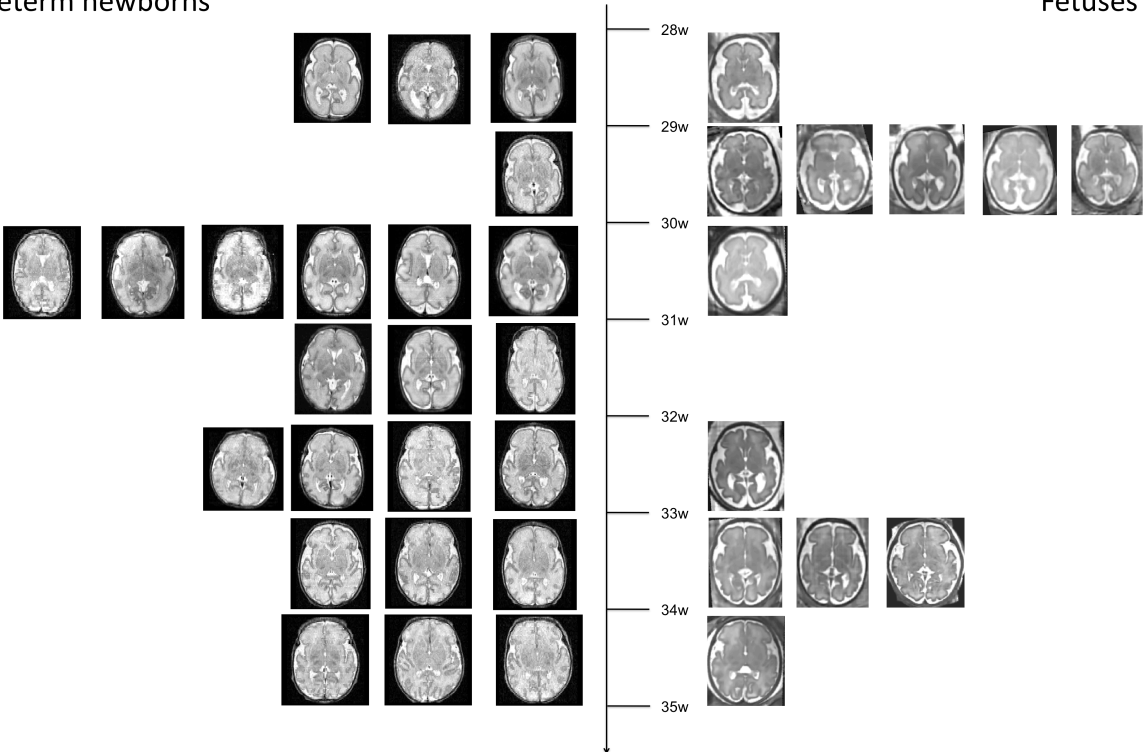
12: Université Paris Diderot, Sorbonne Paris Cité, UMR-S 1161 INSERM, Paris, France

# Supplementary Figure 1

Visual comparison of the MRI for the 23 preterm newborns and 12 fetuses between 28 and 34 gestational age.

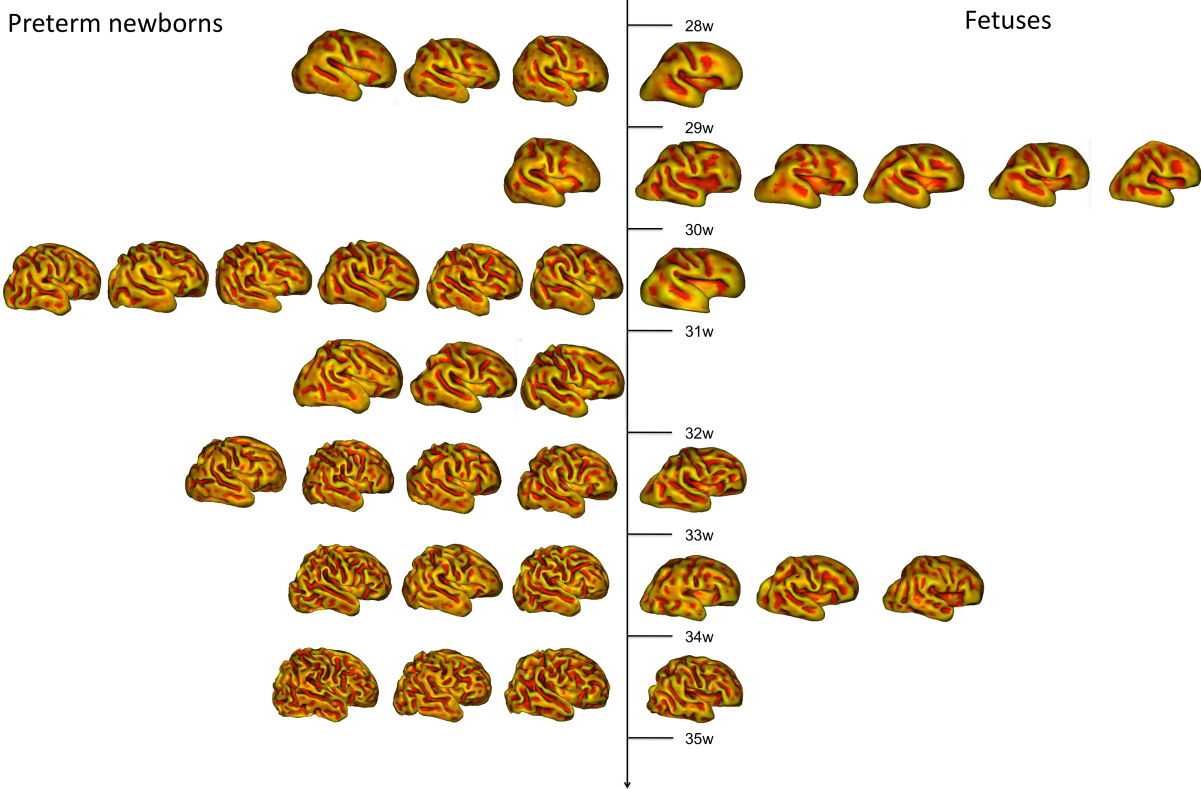
Preterm newborns

Fetuses



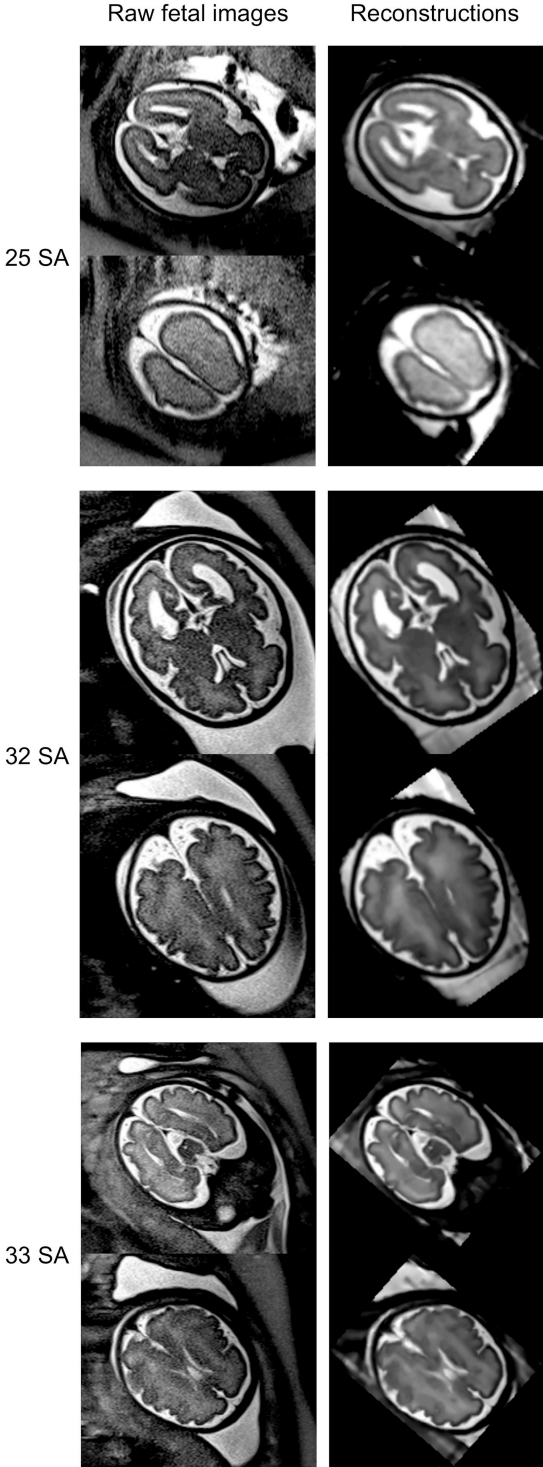
# Supplementary Figure 2

Visual comparison of the cortical surfaces for the 23 preterm newborns and 12 fetuses between 28 and 34 gestational age.



### Supplementary Figure 3

Comparison of raw fetal images and reconstructed images for 3 subjects at various ages. It is clear on those three examples that the reconstruction algorithm did not introduce supplementary blurring.





curvatures. Our measure is also obtained as a peak in a gamma distribution fitting the curvedness while Wright et al simply use the mean of the curvedness.

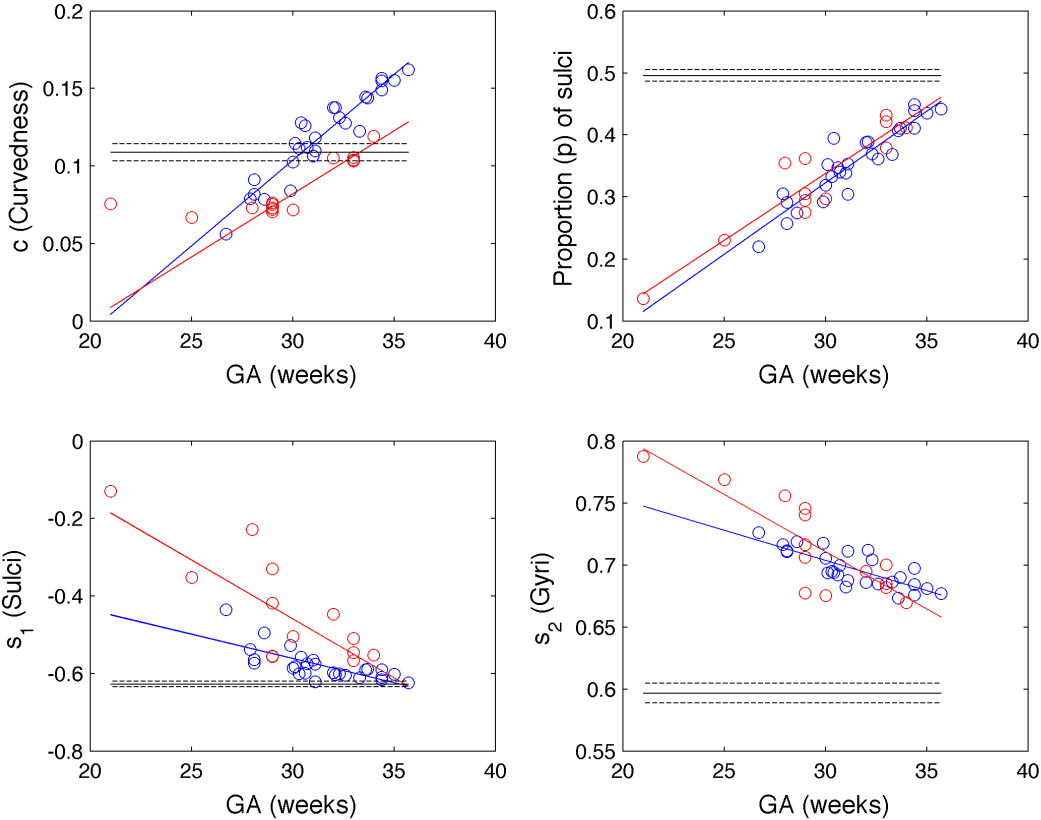
- More interestingly the evolution of the adapted curvedness with GA follows a similar dynamic as what we observe on Fig 9 of Wright et al. On the fetus group, there is a rapid increase at around 25 weeks followed by a linear regime. On the preterm group we observe also a linear regime between 26 and 34 weeks followed by a slowing down at around 35 weeks.

- This figure suggests that using non-linear models such as Gompertz or even sigmoid could probably have a better fit to data. The price to pay is often the increase in the number of parameters to estimate, a higher sensitivity in the regression and a lack of generalized statistical methods.

- Last, the adapted mean curvature allows a better comparison between perinatal values and adult values than without adaptation (see SI Fig 6, top left).



### Supplementary Figure 6



Top left: mean of the peak of the curvedness distribution (black line) computed on the ICBM database with its standard deviation ( $0.108 \pm 0.005$ ).

Top right, bottom left, bottom right: same legend for the proportion of sulci ( $0.50 \pm 0.01$ ), the modes of shape index ( $-0.63 \pm 0.01$ ) and ( $0.60 \pm 0.01$ ) respectively

## Supplementary analysis 1: leverage effects

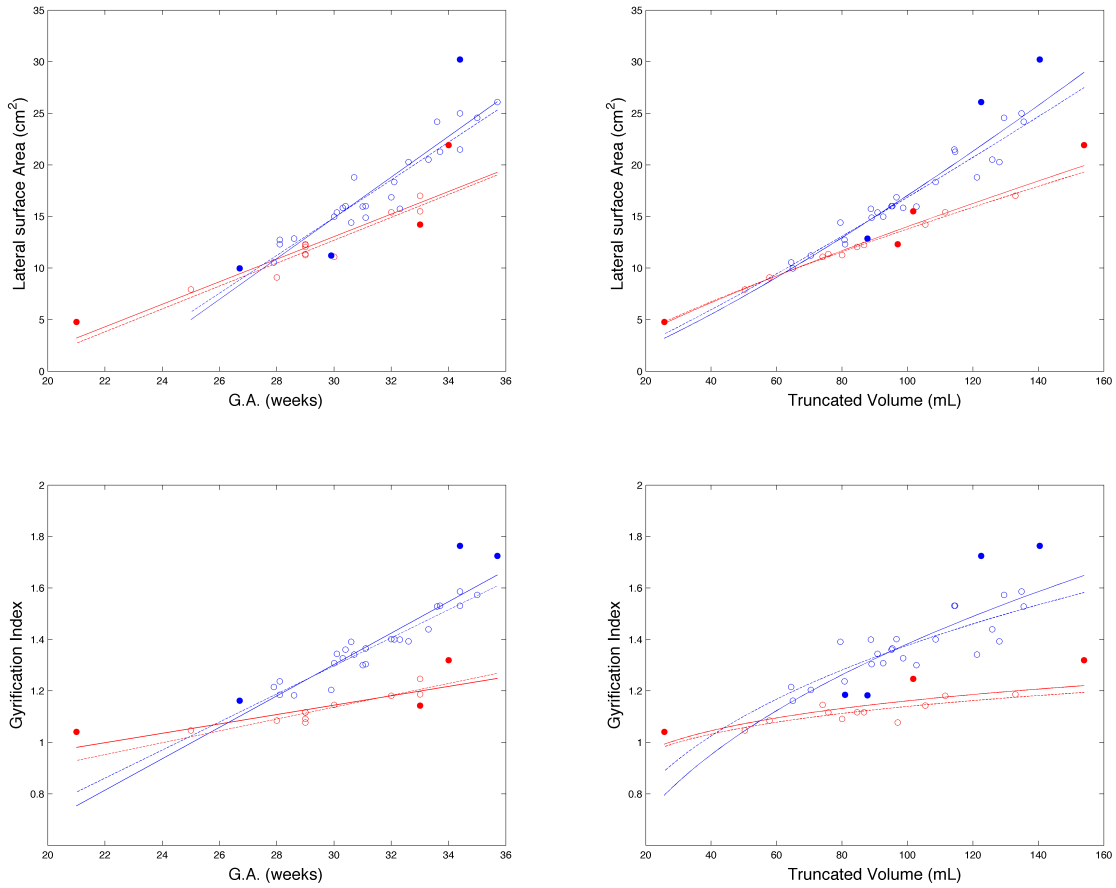
We tested the influence of possible outliers on ANCOVA analysis with the following methodology:

- First we compute Cook's distance for each subject from the regression model (Cook and Weisberg, 1982).
- We removed points whose Cook's distance exceed  $4/n$  where  $n$  is the number of subjects in the considered group (14 or 27 depending on the case) following Bollen and Jackman, 1990.
- We ran another ANCOVA analysis on this reduced dataset.

The methodology was applied for the exterior surface and gyrification index. We provide an updated table of the results and regression plots, with results on the complete dataset

Explained variable	R <sup>2</sup>	Covariables		Group	Interaction
		GA	log(V <sub>tr</sub> )		
S <sub>lat</sub>	0.86	228.2/<.001		10.9/ .002	15.1/<.001
<b>3, 3</b>	<b>0.91</b>	<b>343.6/&lt;.001</b>		<b>20.2/&lt;.001</b>	<b>10.7/0.003</b>
log(S <sub>lat</sub> )	0.96		822.1/<.001	42.3/<.001	27.5/<.001
<b>4, 3</b>	<b>0.96</b>		<b>817.7/&lt;.001</b>	<b>53.6/&lt;.001</b>	<b>19.0/&lt;.001</b>
GI	0.91	255.2/<.001		89.4/<.001	46.1/<.001
<b>3, 3</b>	<b>0.95</b>	<b>429.1/&lt;.001</b>		<b>159.0/&lt;.001</b>	<b>27.9/&lt;.001</b>
log(GI)	0.82		101.0/<.001	60.6/<.001	22.6/<.001
<b>3, 4</b>	<b>0.88</b>		<b>129.5/&lt;.001</b>	<b>107.7/&lt;.001</b>	<b>12.2/.002</b>

Supplementary Table 1 : Details of the statistical analyses: results of the ANCOVA models for the parameters of interest. For each variable, the first line and the second line corresponds to the results found for the entire and reduced dataset, respectively. We show also on the first column the number of fetuses and preterm newborns (separated by a comma) excluded by applying Cook's criterion.



### Supplementary figure 7

Regression plots before and after the exclusion of outliers (solid and dotted lines respectively). Outliers among fetuses and preterm newborns are represented by thick points (red and blue, respectively). From top to bottom, left to right: Lateral surface vs G.A., Lateral Surface vs Volume, Gyrfication Index vs G.A. and Gyrfication vs Volume.

Even if some subjects are systematic outliers, one can note that they do not perturbate the ANCOVA analysis that are highly comparable.

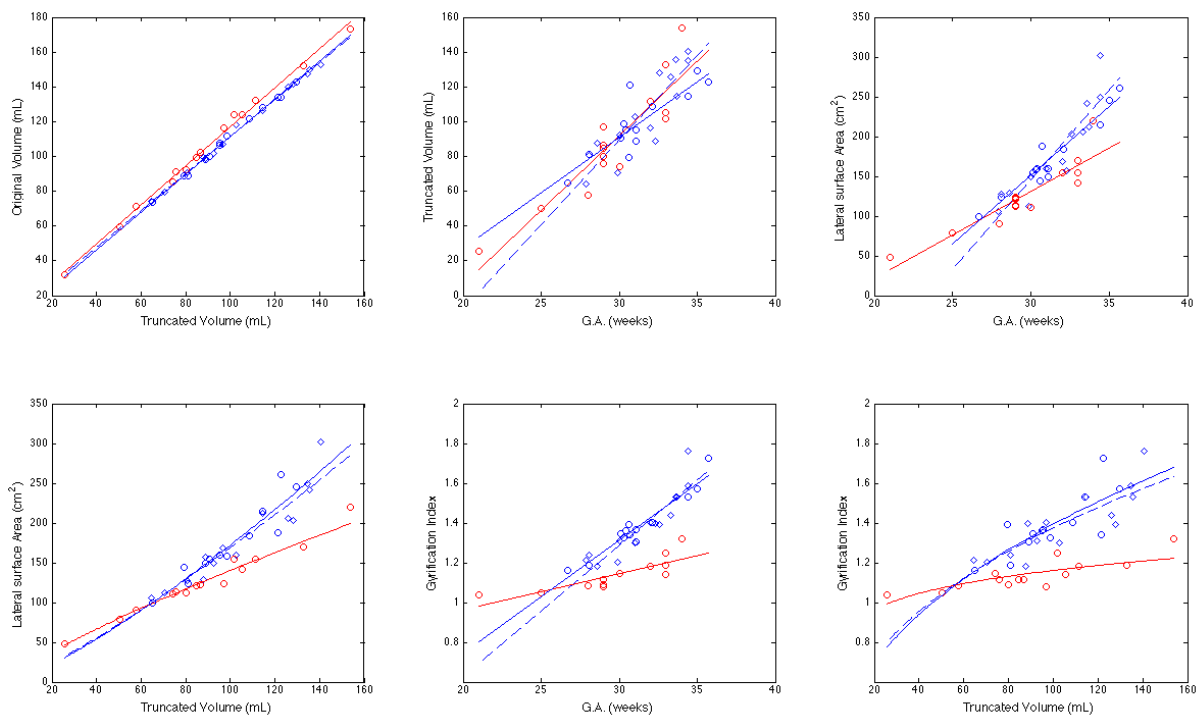
## Supplementary analysis 2: influence of extra-uterine time

We tested the influence of extra-uterine time on the morphometric parameters of figure 4 for preterm newborns. For this, we divided the group in 13 newborns whom age for MRI acquisition time was inferior to 1 week and 14 with an age superior to 1 week.

We displayed regression lines for the two groups of preterms (<1week: blue solid line, >1week: blue dashed line) and the fetuses (red line). We observed qualitatively that our previous results on Figure 4 and supplementary figure 7 were preserved.

We compared the influence of extra-uterine time on the different parameters by using ANCOVA models with the two previous groups of preterms, without considering the fetuses. For all the parameters (Original Volume, Volume, Surface vs GA, Surface vs Volume, GI vs GA, GI vs GA), only independent quantitative variable (Volume, G.A., G.A, Volume, G.A., Volume) had a significant influence. There was no influence of the group variable and no influence of the interaction term.

Those complementary analyses indicated that the extra-uterine time was not a major determinant of the differences observed between fetuses and preterms.



## References

Wright, R., Kyriakopoulou, V., Ledig, C., Rutherford, M.A., Hajnal, J.V., Rueckert, D., Aljabar, P., 2014. Automatic quantification of normal cortical folding patterns from fetal brain MRI. *Neuroimage* 91, 21-32.

Cook, R. Dennis; and Weisberg, Sanford (1982); *Residuals and influence in regression*, New York, NY: Chapman & Hall.

Bollen, Kenneth A.; and Jackman, Robert W. (1990); *Regression diagnostics: An expository treatment of outliers and influential cases*, in Fox, John; and Long, J. Scott (eds.); *Modern Methods of Data Analysis* (pp. 257-91). Newbury Park, CA: Sage